Image Compression with a Hybrid Wavelet-Fractal Coder

Jin Li and C.-C. Jay Kuo

***Abstract*—A hybrid wavelet-fractal coder (WFC) for image compression is proposed in this research. The WFC uses the fractal contractive mapping to predict the wavelet coefficients of the higher resolution from those of the lower resolution and then encode the prediction residue with a bitplane wavelet coder. The fractal prediction is adaptively applied only to regions where the rate saving offered by fractal prediction justifies its overhead. A rate-distortion criterion is derived to evaluate the fractal rate saving and used to select the optimal fractal parameter set for WFC. The superior performance of WFC is demonstrated with extensive experimental results.**

***Index Terms*—Fractal compression, image coding, wavelet compression, wavelet-fractal coder.**

I. Introduction

Fractal compression is distinctive from conventional transform-based coding methods in several aspects [1], [2]. First, rather than directly encoding the image content, fractal coding uses the contractive mapping to represent an image. Second, unlike the invertible transform used in the transform-based coders, contractive mapping is an irreversible procedure. Third, quantization of contractive mapping parameters is not the main source of distortion. The compression artifact is primarily caused by the process of contractive mapping. Thus, the bit rate and image quality control for the fractal coder is difficult to perform. In spite of all achievements in fractal theory and coder implementations, the rate-distortion (R-D) performance of the fractal coder can hardly match the state-of-the-art wavelet coders such as the embedded zerotree wavelet coder (EZW) [3] and the layered zero coder (LZC) [4].

The relationship between fractal and transform-based coders has been recently investigated in [5]–[7]. Rinaldo and Calvagno [6] proposed a predictive pyramid coder (PPC) by exploring the interscale redundancy. PPC performed a block-based interscale prediction, which was independent of each resolution and directional subband, and the block size could be adjusted. It turned out that PPC bore little resemblance to the contractive mapping defined in traditional fractal coders. Davis [7] showed that the fractal contractive mapping could be considered as a prediction operation in the wavelet domain. That is, coefficients of the higher resolution are predicted from those of the lower resolution. The three commonly used spatial fractal operators have their correspondence in the wavelet domain. The averaging and subsampling operator shifts wavelet coefficients to a higher resolution and prunes the coefficients of the highest resolution. The isometry operator permutes the wavelet coefficients within each scale, and the scaling operator multiplies the coefficients by a gain factor. With above observations, a fractal coder in the wavelet domain called the self-quantization of subtrees (SQS) was developed in [7].

Following [7], we use fractal to predict wavelet coefficients of the higher resolution from those of the lower resolution. However, unlike PPC, SQS and other conventional fractal coders, where the whole image is encoded by fractal prediction alone, we encode the fractal prediction residue with a bitplane wavelet coder. Furthermore, we adaptively apply the fractal prediction to a selected part of the image wherever the rate saving of fractal prediction justifies its overhead. An R-D criterion is derived to evaluate the fractal rate saving and used to select the optimal fractal parameter set for WFC. The superior performance of WFC is demonstrated with extensive experimental results.

Manuscript received January 13, 1997; revised July 31, 1998. This work was supported by the Integrated Media Systems Center, a National Science Foundation Engineering Research Center, by the Annenberg Center for Communication of the University of Southern California, and the California Trade and Commerce Agency. The associate editor coordinating the review of this manuscript and approving it for publication was Dr. Christine Podilchuk.

J. Li is with Sharp Laboratories of America, Camas, WA 98607 USA (e-mail: lijin@ sharplabs.com).

C.-C. Jay Kuo is with Integrated Media Systems Center and the Department of Electrical Engineering-Systems, University of Southern California, Los Angeles, CA 90089-2564 USA (e-mail: cckuo@sipi.usc.edu).

Publisher Item Identifier S 1057-7149(99)04056-7.

II. Wavelet Fractal Coder

The proposed WFC is a combination of the adaptive fractal prediction and bitplane wavelet coding. Specifically, we only apply fractal prediction to regions where the fractal rate saving justifies its overhead. Detailed implementations are described below.

A. Step 1: Wavelet Decomposition

The image is decomposed with a two-dimensional (2-D) pyramidal wavelet transform. The biorthogonal 9-7 spline filter with symmetric boundary extension is used in this work. The depth of the wavelet decomposition d is determined by the range block size K through the relationship $d = 1 + \log_2 K$.

B. Step 2: Search for Fractal Prediction

The original image is partitioned into a union of nonoverlapping range blocks. Each range block corresponds to a spatial region of size $K \times K$, and is constituted by three $K/2 \times K/2$ subblocks in resolution 1, three $K/4 \times K/4$ subblocks in resolution $2, \cdots$, and three 1×1 subblocks in resolution $\log_2 K$, where the three subblocks in each resolution reside in the LH, HL, and HH subbands, respectively. Each range block is matched with a domain block which corresponds to a spatial region of size $2K \times 2K$, and is constituted by three $K \times K$ subblocks in resolution 2, three $K/2 \times K/2$ subblocks in resolution $3, \cdots$, and three 1×1 subblocks in resolution $d = 1 + \log_2 K$. Domain subblocks in resolution 1 are not used. Let the position of the range block be the upper-left corner of its resolution 1 subblock, which is denoted by (x_r, y_r), and let the position of the domain block be the upper-left corner of its resolution 2 subblock, which is denoted by (x_d, y_d). We may subsequently derive the upper-left positions of the resolution s range and domain subblocks to be $(2^{s-1} \cdot x_r, 2^{s-1} \cdot y_r)$ and $(2^{s-2} \cdot x_d, 2^{s-2} \cdot y_d)$, respectively. It is apparent that a range and a domain block located at the same spatial location satisfy:

$$x_d = x_r/2 \quad \text{and} \quad y_d = y_r/2. \tag{1}$$

Since exhaustive search of all domain block locations can be computationally intensive, we can restrict matching domain blocks to a neighborhood of the range block defined by a distance parameter *dist*, as follows:

$$|x_d - x_r/2| < \mathit{dist}/2 \quad \text{and} \quad |y_d - y_r/2| < \mathit{dist}/2. \tag{2}$$

Alternatively, we may demand the domain block to be located on a grid pattern

$$x_d \quad \text{and} \quad y_d \text{ are a multiple of } g. \tag{3}$$

In (2) and (3), *dist* and g are two parameters traded between the

TABLE I
WAVELET ISOMETRY OPERATORS

Isometry	Operation	Wavelet Isometry		
		Subblock isometry	Exchange subblocks LH and HL	Sign change for Subblocks:
Identical		Identical	No	None
Horizontal flip		Horizontal flip	No	LH, HH
Vertical flip		Vertical flip	No	HL, HH
Transpose		Transpose	Yes	None
Diagonal flip		Diagonal flip	Yes	LH, HL
90 degree rotation		90 degree rotation	Yes	LH, HH
180 degree rotation		180 degree rotation	No	LH, HL
270 degree rotation		270 degree rotation	Yes	HL, HH

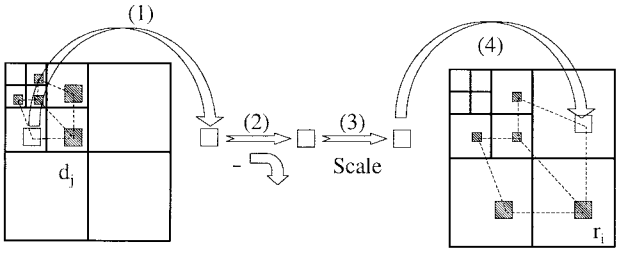

Fig. 1. Illustration showing fractal wavelet prediction for the LH subblock of resolution 1 under the 90° rotation isometry. The prediction operations are carried out as follows. (1) Obtain a matching domain subblock from the HL subband of resolution 2. (2) Rotate 90° and change the sign of all coefficients. (3) Scale the coefficients by a scaling factor. (4) Match with the range subblock at the LH subband of resolution 1.

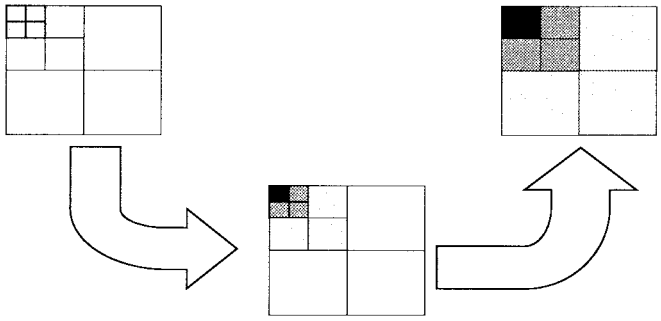

Fig. 2. Framework of the WFC. The blank area has not been encoded yet, the dotted area is currently under the coding process, the meshed area represents the coefficients used for fractal prediction, the black area has already been processed.

fractal search complexity and the fractal prediction efficiency. They affect the number of bits required to encode fractal prediction as well.

The match between range and domain blocks is carried out simultaneously over all resolutions, with a range subblock of resolution s matched with a domain subblock of resolution $s+1$ with the same size. The subblock may undergo wavelet isometry operation Γ. As a result, wavelet coefficients may be modified and may not match with those in the subblock along the same subband direction. For example, if the isometry is a 90° clockwise rotation as shown in Fig. 1, the LH subblock of resolution 1 will match with the negative clockwise rotated HL subblock of resolution 2. There are eight common space-domain isometry operators, i.e., the identical, horizontal flip, vertical flip, transpose, diagonal flip, 90, 180, and 270° clockwise rotation operations. Performed in the wavelet domain, the wavelet isometry operator Γ first shuffles pixels by the same space-domain isometry operator for each wavelet subblock. Then, it may interchange HL and LH subblocks and may switch the sign (multiplied by -1) of some subblocks. (The exact operation of isometry operators in the wavelet domain is summarized in Table I.) Finally, the subblock may be multiplied by a scaling factor α, which is usually quantized with precision Q_α. The fractal search operation finds for each range block its optimal matching domain block with its position (x_d, y_d), isometry operator Γ, and scaling factor α. Exhaustive search is adopted in this work to demonstrate the best possible performance.

C. Step 3: Efficiency Evaluation of Fractal Prediction

The efficiency of fractal prediction is evaluated with an R-D criterion. The perspective coding rates with and without fractal prediction are estimated with respect to a certain quality level and denoted as R_a and R_b, respectively. The rate saving $R_b - R_a$ is compared with the overhead bits R_o required to encode fractal prediction parameters. Fractal prediction is only adopted for those range blocks, which satisfy

$$R_b - R_a > R_o. \tag{4}$$

The status of whether a range block is fractal predicted is arranged in a binary map and encoded with JBIG. For fractal predicted range blocks, parameters including the position of the matching domain block (x_d, y_d), the type of wavelet isometry Γ, and the scaling factor α are encoded and transmitted.

D. Step 4: Wavelet Coding Assisted by Fractal Prediction

WFC proceeds in a top-down fashion with the assistance of the adaptive fractal prediction, as shown in Fig. 2. The coding starts at the lowest resolution d. There is no fractal prediction at this resolution. The four subbands LL, LH, HL, and HH of the resolution d are encoded by a bitplane wavelet coder with a terminal significant threshold T that is calculated from the target image quality PSNR as

$$T = \sqrt{12 D_t}, \quad \text{with } D_t = 255^2 \cdot 10^{-\mathrm{PSNR}/10}. \tag{5}$$

The bitplane coder first quantizes wavelet coefficients by a uniform quantizer with step size T and deadzone $[-T, T]$, and quantized results are bitplane coded by a modified layered zero coder [8]. After the coding of resolution d, the WFC moves to a higher resolution $d-1$. The adaptive fractal prediction is performed for

TABLE II
FRACTAL PARAMETER SELECTION OF GRID SIZE g

Image	Average Rate Saving				
	g=1	2	4	8	16
Barbara	3.85	3.31	1.96	0.65	-0.03
Lighthouse	8.28	7.67	6.47	3.81	1.82
Town	4.26	3.57	2.58	1.72	0.95
Wood	47.24	42.17	35.45	27.10	20.91

TABLE III
FRACTAL PARAMETER SELECTION OF DOMAIN RANGE *DIST*

Image	Average Rate Saving					
	dist=1	2	4	8	16	128
Barbara	-0.98	-0.95	-0.70	-0.44	0.03	3.85
Lighthouse	1.61	3.68	4.46	5.56	6.16	8.28
Town	-0.98	-0.73	-0.22	0.49	1.28	4.26
Wood	1.06	5.86	13.67	21.73	30.43	47.24

those subblocks, which belong to the fractal predicted range blocks. The matching domain subblock in the lower resolution is located and modified according to the wavelet isometry rule, scaled by factor α, and used to predict the current subblock. The prediction residue is further encoded by the bitplane wavelet coder with the same terminal significant threshold T. For the subblock that belongs to the nonfractal predicted range blocks, the prediction value is set as zero and its coefficients are directly encoded by the bitplane wavelet coder. After coefficients of resolution $d-1$ are handled, the WFC proceeds to an even higher resolution $d-2$. The process repeats until coefficients at resolution 1 are encoded.

III. FRACTAL EFFICIENCY EVALUATION AND PARAMETER OPTIMIZATION

We use a rate-distortion criterion to calculate the rate saving of fractal prediction. It is expected that bitplane coding of a subblock of size S and variance σ^2 with terminal threshold T results in the mean square error (MSE)

$$D_t = T^2/12. \tag{6}$$

The total number of coding bits can be calculated as

$$R_t = \frac{S}{\beta}\log_2\frac{\max(\sigma^2, D_t)}{D_t} \tag{7}$$

where β is the coding efficiency parameter usually set to 2.0. Equations (6) and (7) are empirically derived from experiments of a bitplane coder [9]. With (6) and (7), the perspective coding rate before and after the fractal prediction (R_b and R_a) for a bitplane wavelet coder with terminal threshold T can be calculated as

$$\begin{aligned} R_b &= \frac{1}{\beta}\sum_{i=1}^{N} S_i \log_2\frac{\max\left(\sigma_{b,i}^2, D_t\right)}{D_t}, \\ R_a &= \frac{1}{\beta}\sum_{i=1}^{N} S_i \log_2\frac{\max(\sigma_{a,i}, D_t)}{D_t} \end{aligned} \tag{8}$$

where $\sigma_{b,i}^2$ is the variance of the subblock before fractal prediction, $\sigma_{a,i}^2$ is the variance of the subblock after fractal prediction, S_i is the size of the subblock, and $i = 1, \cdots, N$ traverses through all the subblocks in a range block. Note the choice of the terminal threshold T in (5) sets the coding distortion to be the target image quality PSNR.

TABLE IV
FRACTAL PARAMETER SELECTION OF WHETHER USING THE ISOMETRY OPERATORS

Image	Average Rate Saving	
	No isometry	With isometry
Barbara	0.73	3.85
Lighthouse	6.85	8.28
Town	3.49	4.26
Wood	44.24	47.24

TABLE V
FRACTAL PARAMETER SELECTION OF THE QUANTIZATION STEP SIZE OF THE SCALING FACTOR Q_α

Image	Average Rate Saving					
	$Q_\alpha=2^{-2}$	2^{-3}	2^{-4}	2^{-5}	2^{-6}	2^{-7}
Barbara	2.43	3.84	3.85	3.84	3.71	3.56
Lighthouse	6.47	7.71	8.28	8.09	7.99	7.83
Town	1.64	4.15	4.26	4.15	3.87	3.58
Wood	34.30	44.31	47.24	46.93	46.11	45.25

TABLE VI
FRACTAL PARAMETER SELECTION OF THE RANGE BLOCK SIZE K

Image	Average Rate Saving			Total Rate Saving		
	K=8	16	32	K=8	16	32
Barbara	1.39	3.85	2.45	5693	3942	627
Lighthouse	0.54	8.28	27.47	2200	8479	7032
Town	0.58	4.26	4.76	2376	4362	1218
Wood	14.25	47.24	72.27	58368	48373	18501

TABLE VII
UNIVERSAL VERSUS SCALE-BY-SCALE

Image	Average Rate Saving		Total Rate Saving	
	Universal	Scale-by-scale	Universal	Scale-by-scale
Barbara	3.85	0.38	3942	517
Lighthouse	8.28	1.67	8479	2271
Town	4.26	1.26	4362	1714
Wood	47.24	16.54	48373	22494

The perspective coding rate (8) is used to evaluate fractal prediction efficiency as well as to select the optimal parameter set for fractal prediction. This parameter set includes the grid size g, the distant parameter *dist*, the type of isometry, the quantization precision of scaling factor Q_α, and the range-domain block size K. A different fractal parameter set results in different overhead bits for fractal prediction. The optimal fractal prediction parameters are selected through the calculation of the average rate saving, which is defined as the average decrease of the perspective coding rate achieved by fractal prediction per range block:

$$R_s = \frac{1}{N}\left(-N + \sum_{R_b - R_a > R_o} R_b - R_a - R_o\right). \tag{9}$$

TABLE VIII
PSNR RESULTS OF THE LENA IMAGE

Image	Experiment 1		Experiment 2		Experiment 3		Experiment 4		Experiment 5	
	Rate(bpp)	PSNR(dB)	Rate	PSNR	Rate	PSNR	Rate	PSNR	Rate	PSNR
JPEG	-	-	-	-	0.1855	28.61	0.3785	33.34	0.7643	36.68
FRAC	-	-	-	-	0.2175	30.71	0.4477	33.40	0.7626	35.92
PPC	-	-	0.18	31.20	0.26	32.78	0.37	34.00	-	-
SQS	0.0363	25.86	0.0804	28.55	0.1799	31.80	0.3662	34.92	0.7668	38.14
EZW	0.0359	25.79	0.0825	28.66	0.1816	31.76	0.3694	34.93	0.7574	38.11
LZC	0.0359	26.33	0.0825	29.27	0.1816	32.51	0.3694	35.60	0.7574	38.63
WFC	0.0359	26.42	0.0825	29.41	0.1816	32.68	0.3694	35.84	0.7574	39.02

We have taken into consideration in (9) the overhead bits R_o in coding fractal parameters and the one bit overhead per range block, which identifies whether the block is predicted via the fractal prediction rule.

A set of experiments is performed to determine the optimal fractal parameter set. We vary the grid size g among 1, 2, 4, 8, and 16, the distant parameter *dist* among 1, 2, 4, 8, 16 and 128, the quantization precision of scaling factor Q_α among 2^{-2}, 2^{-3}, 2^{-4}, 2^{-5}, 2^{-6}, and 2^{-7}. We also switch on and off the wavelet isometry operator. Our test images are Barbara, lighthouse, town, and wood in the USC image database, all of size 512 $\times$ 512. In each experiment, we tune only one fractal parameter and fix the rest. The default states of these parameters are $g = 1$, *dist* $= 128$, the quantization precision of scaling factor Q_α is 2^{-4}, and the isometry is on. The corresponding results are listed in Tables II–V. We underline parameters corresponding to the maximum average rate saving in each experiment.

According to these experimental results, the following parameters are chosen for WFC.

- The optimal grid size g is 1.
- The optimal search range *dist* for the domain block is 128, which is the maximum, since the size of a resolution 2 subband in the 512 $\times$ 512 image is 128 $\times$ 128.
- The use of the isometry operation improves fractal prediction efficiency.
- The optimal quantization precision for scaling factor Q_α is 2^{-4}.

Compared with traditional fractal coders [1], [2], where a grid size g of 4 or 8 is considered as optimum, a much more refined grid is optimal in the WFC. Since fractal prediction is only used in fractal efficient regions in the WFC, there is no need to compromise the value of g for fractal inefficient regions. This choice, however, increases the fractal search complexity. The above fractal parameter set maximizes the rate saving. It is also possible to select parameters with the computational complexity in consideration. Again, we use the average rate saving to guide the parameter selection. For example, we may choose to increase the grid size from $g = 1$ to $g = 8$, which decreases the computational complexity by a factor of 64 and results in a loss of an average rate saving of 7.59 bits according to Table II. Similarly, we can reduce the domain block search range from *dist* $= 128$ to *dist* $= 16$, which also decreases the search complexity by a factor of 64 while increasing the coding rate by an average of 6.43 bits per range block according to Table III. We may chose to eliminate the isometry operator, which decreases the search complexity by a factor of 8 and loses an average rate saving of 2.08 bits as shown in Table IV. Apparently, if the computational complexity is critical, we should first eliminate isometric operators, then decrease the domain search range and finally increase the grid size. With this sequence, we can reduce the computational complexity while minimizing the loss in fractal prediction efficiency. An alternative way to reduce the fractal search complexity is using a fast fractal search algorithm [5]. No matter whether the complexity is reduced by using fast fractal search or downsizing the domain pool, the R-D performance of WFC degrades with a lower search complexity. It is therefore a compromise between the coder complexity and the R-D performance.

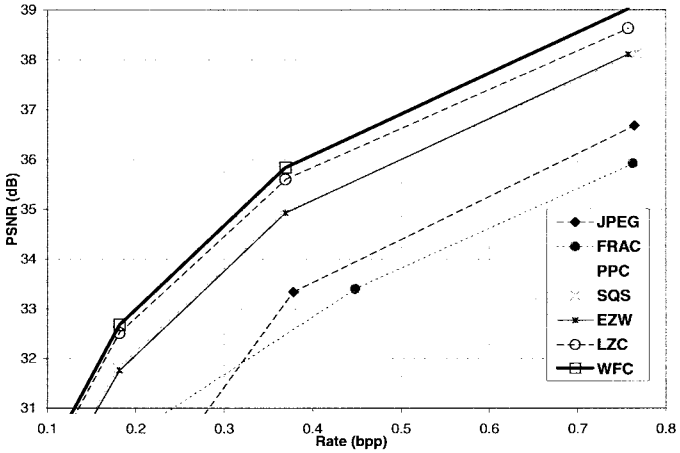

Fig. 3. PSNR performance comparison of coding algorithms for image Lena.

The rate-distortion criterion can also be used to select the optimal range block size K, and experimental results are shown in Table VI. Since the number of range blocks decreases as the size of the block increases, we show, in addition to the average rate saving R_s the total rate saving R_{total} in Table VI with

$$R_{\text{total}} = R_s \cdot N. \tag{10}$$

It can be observed that the optimal range block size K is either 8 or 16. For the four test images, losses in total rate savings of using the block size $K = 8$ versus $K = 16$ are 74% and 46% for lighthouse and town, while losses in rate savings of using block size $K = 16$ versus $K = 8$ are 31% and 17% for Barbara and wood, respectively. The range block size K is thus chosen to be 16 for the robust reason.

Finally, we investigate a scheme where fractal prediction is independent of each resolution, which is more or less similar to the PPC in [6]. In such a scheme, a range block of resolution s (consisting of three $K/2 \times K/2$ subblocks from the LH, HL, and HH subbands of resolution s) is matched with a domain block of resolution $s+1$ (consisting of three $K/2 \times K/2$ subblocks from the LH, HL, and HH subbands of resolution $s+1$). We call such an approach the scale-by-scale fractal prediction and the previous approach the universal scale fractal prediction. Performance comparison in terms of the average and total rate savings is shown in Table VII. We again underline the

Fig. 4. Results of the Lena image with (a) JPEG (0.38 b/pixel, 33.34 dB), (b) SQS (0.37 b/pixel, 34.92 dB), (c) LZC (0.37 b/pixel, 35.59 dB), (d) WFC (0.37 b/pixel, 35.84 dB), (e) original, and (f) fractal predicted regions (marked with circled plus sign).

parameter set which offers a better rate saving. The result supports that fractal prediction is highly correlated across scales, and the universal scale fractal prediction is more efficient than that of the scale-by-scale fractal prediction.

TABLE IX
PERFORMANCE COMPARISON BETWEEN LZC AND WFC

Image	Experiment 1		Experiment 2		Experiment 3		Experiment 4		Experiment 5	
	Rate(bpp)	PSNR(dB)	Rate	PSNR	Rate	PSNR	Rate	PSNR	Rate	PSNR
					Image Lena					
LZC	0.0359	26.33	0.0825	29.27	0.1816	32.51	0.3694	35.60	0.7574	38.63
WFC	0.0359	26.42	0.0825	29.41	0.1816	32.68	0.3694	35.84	0.7574	39.02
					Image Barbara					
LZC	0.0353	22.84	0.1335	25.24	0.3351	29.46	0.6679	33.98	1.1761	38.55
WFC	0.0353	22.88	0.1335	25.82	0.3351	29.90	0.6679	34.19	1.1761	38.77
					Image Lighthouse					
LZC	0.0508	22.74	0.1457	25.79	0.3322	29.59	0.6743	34.02	1.2163	38.53
WFC	0.0508	23.19	0.1457	26.40	0.3322	30.18	0.6743	34.26	1.2163	38.76
					Image Town					
LZC	0.0702	19.44	0.2040	22.36	0.5136	26.15	1.0211	30.91	1.7566	36.11
WFC	0.0702	19.56	0.2040	22.53	0.5136	26.56	1.0211	31.17	1.7566	36.25
					Image Wood					
LZC	0.0747	14.86	0.2173	17.99	0.5775	21.55	1.1882	26.79	2.1581	32.15
WFC	0.0747	15.19	0.2173	18.09	0.5775	22.30	1.1882	26.92	2.1581	32.20
					Image Baboon					
LZC	0.0168	19.57	0.0865	21.05	0.3504	23.96	0.8935	27.86	1.7706	32.94
WFC	0.0168	19.55	0.0865	21.15	0.3504	24.24	0.8935	28.39	1.7706	33.46

IV. EXPERIMENTAL RESULTS

The performance of the proposed WFC has been compared with several typical fractal and wavelet coders. They include the block-based fractal coder (FRAC) [2], the PPC [6], the SQS with the biorthogonal wavelet and zerotree coding [7], the EZW [3], and the layered zero coder (LZC) [4]. We also show results of JPEG as a reference. The test images used in the experiment is the Lena of size 512 $\times$ 512. Experimental results of FRAC and PPC are directly taken from [2, Table II] and [6, Fig. 8], respectively. PSNR results are shown in Table VIII and the comparing R-D curves are plotted in Fig. 3. The performance of FRAC is not good even compared with JPEG. Although it outperforms JPEG at low bit rates, it is inferior to JPEG at the middle to high bit rate range. PPC is substantially better than JPEG, but it can hardly compete with the state-of-the-art wavelet coders such as EZW or LZC. By using the biorthogonal wavelet and zerotree, the SQS has a performance similar to EZW but still inferior to LZC. The proposed WFC demonstrates a superior performance in comparison with all other coders. It outperforms LZC by 0.1–0.4 dB, EZW by 0.6–0.9 dB, SQS by 0.5–0.9 dB, PPC by 1.5–2.0 dB, JPEG by 2.3–4.0 dB, and FRAC by 2.0–3.1 dB.

Subjective comparisons of the coded Lena images at 0.37 b/pixel are shown in Fig. 4. For clarity, only the central portion of Lena is shown. The result of JPEG has the blocking artifact at 0.38 b/pixel and is of relatively low quality. The subjective qualities of SQS, LZC and WFC coded Lena at 0.37 b/pixel are close, and are much better than that of JPEG. Careful comparison between SQS and WFC shows that the WFC-coded Lena has a little more texture patterns in the hat. Comparison between LZC and WFC shows that the LZC coded Lena has more ringing artifacts and a few isolated ripples (caused by isolate wavelet coefficients) in the face region.

The fractal predicted range blocks are marked with $\oplus$ sign in Fig. 4(f). It can be observed that fractal efficient regions are usually with high intensity edges or textures. At the coding rate of 0.37 b/pixel, approximately 8% of the entire image region in Lena benefits from the use of fractal prediction. However, fractal efficient regions are usually the ones that consume more bits (e.g. the 8% fractal efficient region consumes 17% of total coding bits).

In the second set of experiments, we perform a more thorough comparison of WFC and LZC, which is the wavelet residue coder of WFC. Our objective is to investigate the performance gain of fractal prediction. Experiments are performed on Lena, Barbara, baboon, wood, town and lighthouse, and results are shown in Table IX. In general, the gain of WFC over LZC is in the range of 0.0 to 0.8 dB, with an average gain of 0.3 dB. The actual gain depends on the characteristics of the image and the operating bit rate. The gain is more for images with many textures and encoded at a higher bit rate. It is worthwhile to point out that there is only one case among 30 comparisons (i.e., baboon image coded at 0.0168 b/pixel) that WFC is inferior to LZC by 0.02 dB. For all other 29 cases, WFC outperforms LZC. Therefore, fractal prediction does provide a consistent performance improvement for the wavelet coder in use.

REFERENCES

[1] A. E. Jacquin, "Image coding based on a fractal theory of iterated contractive image transformations," *IEEE Trans. Image Processing*, vol. 1, pp. 18–30, Jan. 1992.

[2] E. W. Jacobs, Y. Fisher, and R. D. Boss, "Image compression: A study of the iterated transform method," *Signal Processing*, vol. 29, pp. 251–263, 1992.

[3] J. Shapiro, "Embedded image coding using zerotrees of wavelet coefficients," *IEEE Trans. Signal Processing*, vol. 41, pp. 3445–3462, Dec. 1993.

[4] D. Taubman and A. Zakhor, "Multirate 3-D subband coding of video," *IEEE Trans. Image Processing*, vol. 3, pp. 572–588, Sept. 1994.